Journal of Vacuum Science and Technology B

RESEARCH ARTICLE | AUGUST 26 2024

Effect of sputter power on red-shifted optoelectronic properties in magnetron sputtered Ag/ZnO thin films

GuruSampath Kumar A. ; Mahender C. ; Mahesh Kumar U. ; Obulapathi L. ; HemaChandra Rao B. ; Yamuna P. ; Thirupathi A. ; SomaSundar L. N. V. H. ; Venkata Ramana G.

J. Vac. Sci. Technol. B 42, 054002 (2024)
https://doi.org/10.1116/6.0003813

26 August 2024 13:47:53

AVS

JVST B
Journal of Vacuum Science & Technology B

ARTICLE

pubs.aip.org/avs/jvb

Effect of sputter power on red-shifted optoelectronic properties in magnetron sputtered Ag/ZnO thin films

Cite as: J. Vac. Sci. Technol. B **42**, 054002 (2024); doi: 10.1116/6.0003813
Submitted: 12 June 2024 · Accepted: 2 August 2024 ·
Published Online: 26 August 2024

View Online

Export Citation

CrossMark

GuruSampath Kumar A.,[1,a)] Mahender C.,[2] Mahesh Kumar U.,[3] Obulapathi L.,[4] HemaChandra Rao B.,[1] Yamuna P.,[5] Thirupathi A.,[5] SomaSundar L. N. V. H.,[6] and Venkata Ramana G.[7]

AFFILIATIONS

[1]Department of H&S (Physics), Gokaraju Rangaraju Institute of Engineering & Technology, Bachupally, Hyderabad, Telangana 500090, India
[2]Department of Chemistry, Institute of Aeronautical Engineering, Dundigal, Hyderabad, Telangana 500043, India
[3]Department of H&S (Physics), Srinivasa Ramanujan Institute of Technology, Anantapur, Andhra Pradesh 515701, India
[4]Department of H&S (Physics), Annamacharya University, Rajampet, Andhra Pradesh 516126, India
[5]Department of Physics, Malla Reddy Engineering College, Hyderabad, Telangana 500100, India
[6]Department of Basic Sciences (Physics), G. Narayanamma Institute of Science and Technology (Women), Shaikpet, Hyderabad, Telangana 500104, India
[7]Department of Physics, SCNR Government Degree College, Proddatur, YSR Kadapa District, Andhra Pradesh 516360, India

[a)]**Author to whom correspondence should be addressed:** sampathkumar.physics@gmail.com

26 August 2024 13:47:53

ABSTRACT

This study explores Ag/ZnO thin films on glass (Corning 0211) substrates, which were deposited using dc/rf magnetron reactive sputtering at varying Ag-sputter powers. The impact of Ag-sputter power on physical properties, such as structural, surface, compositional, optical, and electrical properties, is systematically explored. Grazing angle x-ray diffraction affirms a single-phase hexagonal wurtzite ZnO structure in all films, predominantly oriented along (002) normal to the substrate. Thin films deposited at 90 W Ag-sputter power exhibit superior structural and morphological properties, including greatest crystallite and grain size, minimum stress, and roughness. Electrical studies indicate that the material exhibits a semiconducting nature, with its electrical resistivity decreasing to a minimum of 0.8 Ω cm at 95 W. At this level of Ag sputter power, the films demonstrate low resistivity, high mobility ($0.49\ cm^2/V\ s$), a charge carrier concentration of $9.6 \times 10^{19}\ cm^{-3}$, and an optical transmittance of 79%, along with an optical band gap energy (Eg) of 3.06 eV. This underscores the influence of Ag sputter power in tailoring Ag/ZnO thin films for optoelectronic applications.

Published under an exclusive license by the AVS. https://doi.org/10.1116/6.0003813

I. INTRODUCTION

The increasing demand for optoelectronic devices, such as thin film transistors, intelligent (smart) windows, flat panel displays, transparent electronic devices, and photovoltaic devices, emphasizes the significance of various process parameters in determining the ultimate performance of these devices. High transparency, cost-effectiveness, nontoxicity, and chemical stability are inherent traits of this material under hydrogen plasma conditions. Furthermore, ZnO films can be deposited at lower temperatures.[1] The electrical characteristics of ZnO are influenced by intrinsic defects, such as zinc interstitials and/or oxygen vacancies. The incorporation of impurities for modifying ZnO properties is presently a significant consideration for potential practical uses.[2] The structural, microstructural, optical, and electrical properties of Ag/ZnO thin films are influenced not only by the deposition technique, but also by the specific synthesis parameters[3,4] utilized employed during their preparation. Several physical and chemical vapor deposition methods have been employed for the fabrication of Ag/ZnO thin films.[5] Among these techniques, dc-magnetron

Published under an exclusive license by the AVS

sputtering stands out as a highly favorable and industrially viable method, particularly for large-area deposition. This technique facilitates the creation of homogeneous films with the desired thickness and excellent adhesion, making it a preferred choice in the industry.[6,7]

In general, the characteristics of films, including their structure, optical, and electrical properties, are significantly influenced by the parameters involved in the deposition process. The electrical behavior of Ag/ZnO thin films demonstrates a correlation with both sputter power and deposition time. Notably, sputter power stands out as a crucial parameter that fundamentally governs the properties of Ag/ZnO films. Elevated sputter power contributes to heightened surface mobility, resulting in the formation of larger crystallite sizes.[8–10] This outcome is attributed to the increased adatom energy, leading to the production of highly crystalline Ag/ZnO films. According to Ramadan *et al.*,[11] dc-magnetron cosputtered Ag/ZnO thin films show enhanced crystallinity and optical transmittance as the sputter power of Ag increases. Hence, sputter power plays a pivotal role in influencing the nucleation, growth, as well as the physical (structural, electrical, and optical) characteristics of Ag/ZnO films. Employing reactive magnetron sputtering, the deposition of Ag/ZnO thin films onto glass substrates can be achieved under diverse growth conditions.[12] Once the partial pressures of the working gas (O_2) and the sputter gas (Ar) have been set, regulating the flow of the nonreactive gas enables the balancing of sputter power supplied to the stationary Zn and Ag targets during the reactive sputtering process. In this study, we synthesized Ag/ZnO thin films using dc/rf magnetron sputtering and investigated the effect of Ag sputter power primarily on the physical properties (structural, electrical, and optical) of ZnO.

II. EXPERIMENTAL DETAILS

Zn-Ag metals with a purity of 99.999% were used as sputtering targets in the reactive dc magnetron sputtering process to create thin layers of Ag/ZnO on crown glass substrates. The deposition chamber was evacuated using a diffusion pump in conjunction with a rotary pump to reach a chamber (base) pressure of 8.5×10^{-6} mbar. High purity Ar and O_2 were introduced as sputter and reactive gases, respectively, using different mass flow controllers. During sputtering, a total pressure of 6×10^{-3} mbar was maintained. The distance between the target and substrate was set at 50 mm. For every sample, the deposition process lasted 20 min.[13] The Zn and Ag targets were presputtered in an argon environment for 10 min before to the deposition of each film in order to clean the target surface of impurities. The process parameters for the deposition of desired Ag/ZnO thin films by dc/rf magnetron sputtering are given in Table I.

Glancing angle x-ray diffraction (Brucker-D8) with Cu-K_α radiation was used to examine the films' crystallinity. The angle 2θ was adjusted in a step of 0.02° between 20 and 80°. Surface morphology and topography were assessed through the utilization of field-emission scanning electron microscopy (FESEM) and atomic force microscopy (AFM). The optical interference technique was used to measure the thickness of the films. A UV-vis-NIR spectrophotometer (Hitachi U-3400) was used to examine the optical characteristics, such as transmittance, band gap, extinction coefficient, etc., of Ag/ZnO thin films at various sputter powers of Ag (0, 90, 95, and 100 W, respectively). Since a comparable glass was used as a reference when measuring transmittance, the transmittance spectra were exclusive to the films. The widely recognized method (the Swanepoel method[14]) was used to compute the refractive index from the optical transmittance data. The electrical properties of Ag/ZnO thin films, encompassing parameters, such as electrical resistivity (ρ), carrier mobility (μ), and concentration (n), were evaluated utilizing the Ecopia HMS-3000 system in a Van der Pauw configuration under ambient conditions and a magnetic field of 0.5 T.

TABLE I. Process parameters for dc/rf magnetron sputtered Ag/ZnO thin films. This table lists the specific conditions and settings used during the deposition process, including sputter power, deposition time, and substrate temperature.

Parameter	Specifications
Sputtering targets	Zn (Purity:4 N) & Ag (Purity: 4 N)
Base (chamber) pressure	8.5×10^{-6} mbar
Base material/substrate	Corning 0211 glass
Sputtered and reactive gases	Ar (5N) & O_2 (4N)
Target to substrate distance	50 mm
Sputter power (zinc)	100 W
Sputter power (silver)	0, 90, 95, and 100 W
Sputtering time	20 min
Flow rates (Ar and O_2)	28 and 2 sccm
Deposition (working) pressure	0.06–0.08 mbar

III. RESULTS AND DISCUSSION

The grazing angle x-ray diffraction (GAXRD) patterns of Ag/ZnO films coated at different Ag-sputter power [Ps(Ag)] on

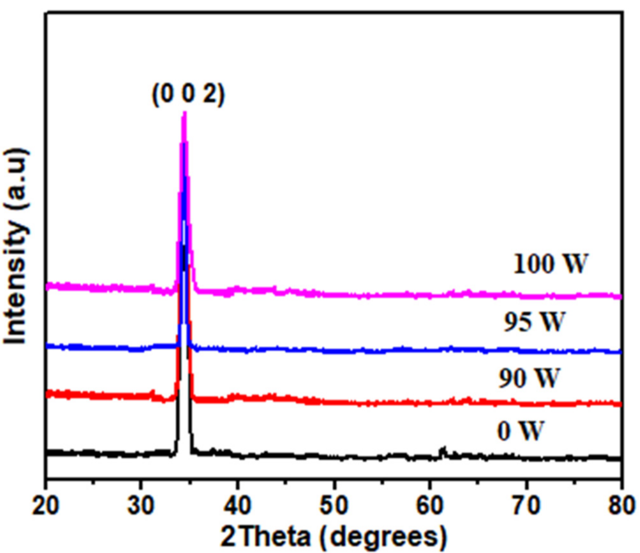

FIG. 1. GAXRD patterns of Ag/ZnO thin films at different Ag-sputter powers [Ps (Ag)]. The patterns illustrate how the crystalline structure of the films evolves with varying Ag deposition conditions.

26 August 2024 13:47:53

Published under an exclusive license by the AVS

TABLE II. Effects of Ag-sputter power [Ps(Ag)] on the full width at half maximum (FWHM), d-spacing, c-constant, crystallite size, stress, and dislocation density in Ag/ZnO thin films. This table summarizes the influence of varying sputter powers on the structural properties of the thin films.

Sputter power [Ps(Ag)] (W)	2θ (deg)	FWHM (deg)	*d*-spacing (nm)	*c*-constant (nm)	Crystallite size (*D*) (nm)	Residual stress (GPa)	Density (disloc.) (cm^{-2})
0	34.55	0.240	0.250	0.5183	41.65	0.544	6.24×10^{14}
90	34.45	0.195	0.258	0.5194	48.63	0.416	4.06×10^{14}
95	34.40	0.168	0.267	0.5202	53.52	0.024	3.46×10^{14}
100	34.48	0.198	0.259	0.5192	43.53	0.343	5.72×10^{14}

glass substrates are shown in Fig. 1. Depending on the Ag-concentration, only the (002) peak at approximately 34.50° is visible in the above GAXRD plot. This observation unambiguously points to a single-phase film with a hexagonal wurtzite ZnO structure; no significant Ag-phase growing is visible. The (002) peak shifts toward lower angles as the Ag-sputter power increases, which is most likely caused by the relatively bigger Ag^{2+} ions (0.93 Å) replacing Zn^{2+} (0.74 Å). The full width at half maximum (FWHM) of the films reduces with increasing Ag-sputter power, indicating an improvement in crystallinity of the films.[15] Thus, the x-ray diffraction patterns show that Ag-sputter power enhances crystallinity, consistent with the findings of Ning *et al.*[16] The improvement is attributed to the increased mobility of adatoms deposited on the surface, a critical factor in forming highly crystalline films. However, Ag/ZnO thin films deposited with 100 W Ag-sputter power show a slight reduction in the grain development and an increase in FWHM due to the significant presence of Ag, which causes distortion. This finding enhances our understanding of the structural changes in the Ag/ZnO system when a substantial amount of Ag is present.

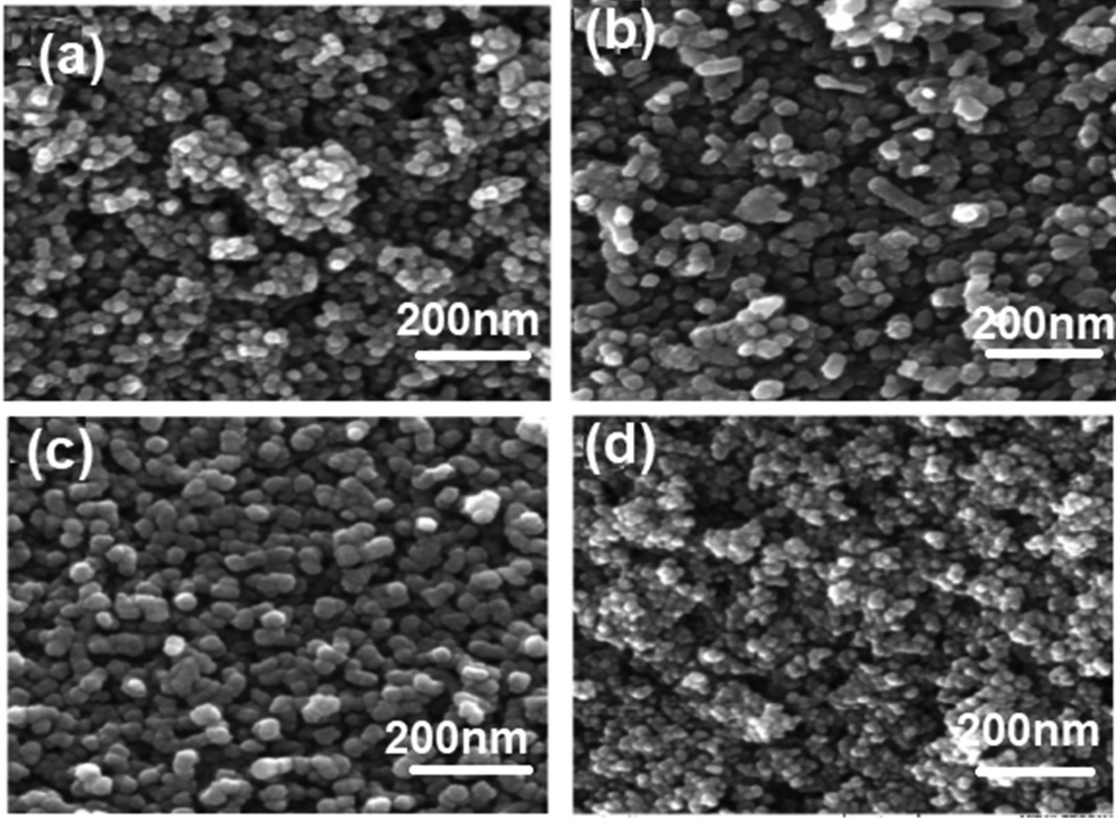

FIG. 2. FESEM images of Ag/ZnO thin films deposited at different Ag-sputter powers: (a) Ps(Ag) = 0 W, (b) Ps(Ag) = 90 W, (c) Ps(Ag) = 95 W, and (d) Ps(Ag) = 100 W. The images show the surface morphology changes with increasing sputter power.

26 August 2024 13:47:53

Published under an exclusive license by the AVS

The determination of the crystallite size (D) in Ag/ZnO thin films was conducted by evaluating the FWHM of the x-ray diffraction peak associated with (002) using Debye–Scherrer's formula,[17] as expressed in Eq. (1),

$$D = \frac{0.94\lambda}{\beta \cos \theta}. \quad (1)$$

Table II shows how the FWHM, d-spacing, c-constant, D, residual stress, and dislocation density change as Ag-sputter power varies. The crystallite size grew from 41.65 to 53.52 nm when the Ag-sputter power increased from Ps(Ag) = 0–95 W. This increase in D with Ps(Ag) suggests that greater surface mobility, caused by increased adatom energy, improves the crystallinity of Ag/ZnO films up to 95 W of Ag-sputter power. Beyond this threshold, a slight reduction in D was found, possibly due to the negative impact of an excessive amount of Ag on film crystallinity, implying lattice distortion.[18]

The c-constant, as indicated in Table II, exhibits minimal variation at low Ag-sputter powers up to 95 W. This is due to the near ionic radii of Ag^{2+} (0.93 A°) and Zn^{2+} (0.74 A°).[19] The residual stress, also detailed in Table II, displays variability with Ag-sputter power, with all films characterized by residual stresses. Notably, the Ag/ZnO film at 95 W Ag-sputter power demonstrated the minimum residual stress at 0.024 GPa. The dislocation density (δ) provides insights into the number of defects in Ag/ZnO thin films, calculated as $\delta = 1/D^2$.[20] Films grown at Ps(Ag) = 95 W exhibited a relatively low dislocation density ($\delta = 3.46 \times 10^{14}\ cm^{-2}$), indicating fewer defects compared to other conditions.

The Ag/ZnO thin film surface characteristics are highly dependent on one of the important deposition parameter called sputter power.[21] FE-SEM pictures of Ag/ZnO thin films at different Ag-sputter powers (0, 90, 95, and 100 W) are shown in Fig. 2. Interestingly, the grain size increases as Ag-sputter power is raised to 95 W, which is consistent with a pattern shown in the GAXRD results (Fig. 1). Numerous studies have emphasized the nanostructural characteristics associated with such crystallite sizes.[22,23] As depicted in Fig. 2, the aggregate size shows consistent augmentation with Ag sputter power up to 95 W. The reason for this phenomenon is that Ag^{2+} (0.93 Å) has a greater ionic radius than Zn^{2+} (0.74 Å). The figures highlight that all films exhibit a smooth, homogeneous surface morphology characterized by spherical nanocrystalline grains. Additionally, the films demonstrate density and strong adhesion to the substrate, devoid of any cracks.[24] The FE-SEM image at 100 W Ps(Ag) is noteworthy because it shows smaller grains than at Ps(Ag) = 95 W. This observation suggests that increased Ag-sputter power has a detrimental effect on the film's crystallinity, which degrades the structural integrity of the film.

AFM pictures of Ag/ZnO thin films formed at various Ag-sputter powers are shown in Fig. 3. These pictures, which encompassed a $3 \times 3\,\mu$m region, provide insight into the grain development and surface textures of Ag/ZnO thin films that were deposited at 0, 90, 95, and 100 W. Notably, the AFM micrographs reveal that crystallite dimensions are confined to the nanoscale, approximately ranging from 30 to 50 nm. The trend in the crystallite size as found by GAXRD analysis is comparable with the AFM image analysis, which shows a modest rise in grain size with the increasing Ag-sputter power (up to 95 W). This implies that the increased Ag-atom incorporation tends to inhibit grain growth, leading the grain size reduction at 100 W.[19] AFM investigations reveal that, up to 95 W of Ag-sputter power, the root mean square (RMS) roughness diminishes. The average surface roughness (RMS) of samples with Ag-sputter power ≤95 W is found to be approximately 13 nm. However, the surface roughness increases noticeably at higher Ag-sputter powers.

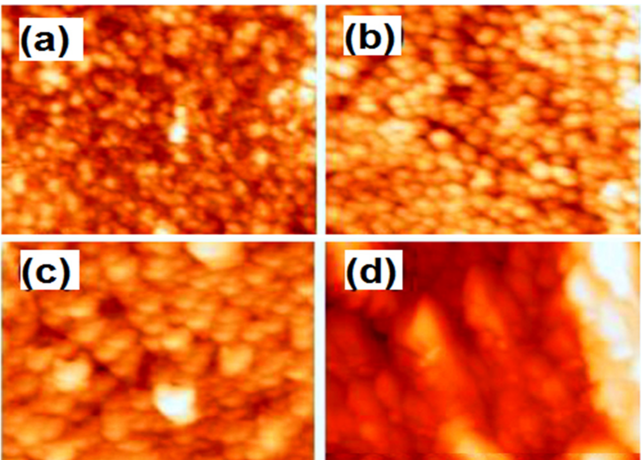

FIG. 3. AFM images of Ag/ZnO thin films as a function of Ag-sputter power: (a) 0, (b) 90, (c) 95, and (d) 100 W. The images depict the surface topography changes with varying Ag-sputter powers.

The investigation of the elemental composition was done via Energy Dispersive x-ray Spectroscopy (EDX). The Ag/ZnO thin film EDX patterns at different Ag-sputter powers are shown in Fig. 4. Zn, O, and Ag-elements were confirmed to be present in the deposited films by EDX analysis. The substrate (glass) is probably the cause of the silicon found in the EDX pattern (Fig. 4). The results displayed in Fig. 4(a) indicated that the sample contained Zn and O elements; with an Ag-sputter power of 0 W (i.e., pristine ZnO), no additional elemental peaks (i.e., Ag) were seen in Ag/ZnO thin films. On the other hand, Figs. 4(b)–4(d), which represent Ag/ZnO thin films with Ag-sputter powers of 90, 95, and 100 W, show that the peaks at 1.185, 0.864, and 3.546 keV, respectively, are linked to Zn, O, and Ag. Interestingly, a rise in Ag-sputter power is correlated with an increase in Ag content in the solid films.[25]

The performance of our synthesized Ag/ZnO thin films can be evaluated by comparing the results of this study with those from previously published works, as shown in Table III.

The optical transmittance, absorption coefficient, energy bandgap, and the location of defect states resulting from contamination of transparent material are all determined using UV-Vis spectroscopy. Figure 5 shows the optical transmittance, which spans the wavelength range of 200–800 nm. Ag/ZnO thin films were observed to have great transparency in the visible spectrum and low transmission in the UV spectrum. Specifically, an increase

26 August 2024 13:47:53

Published under an exclusive license by the AVS

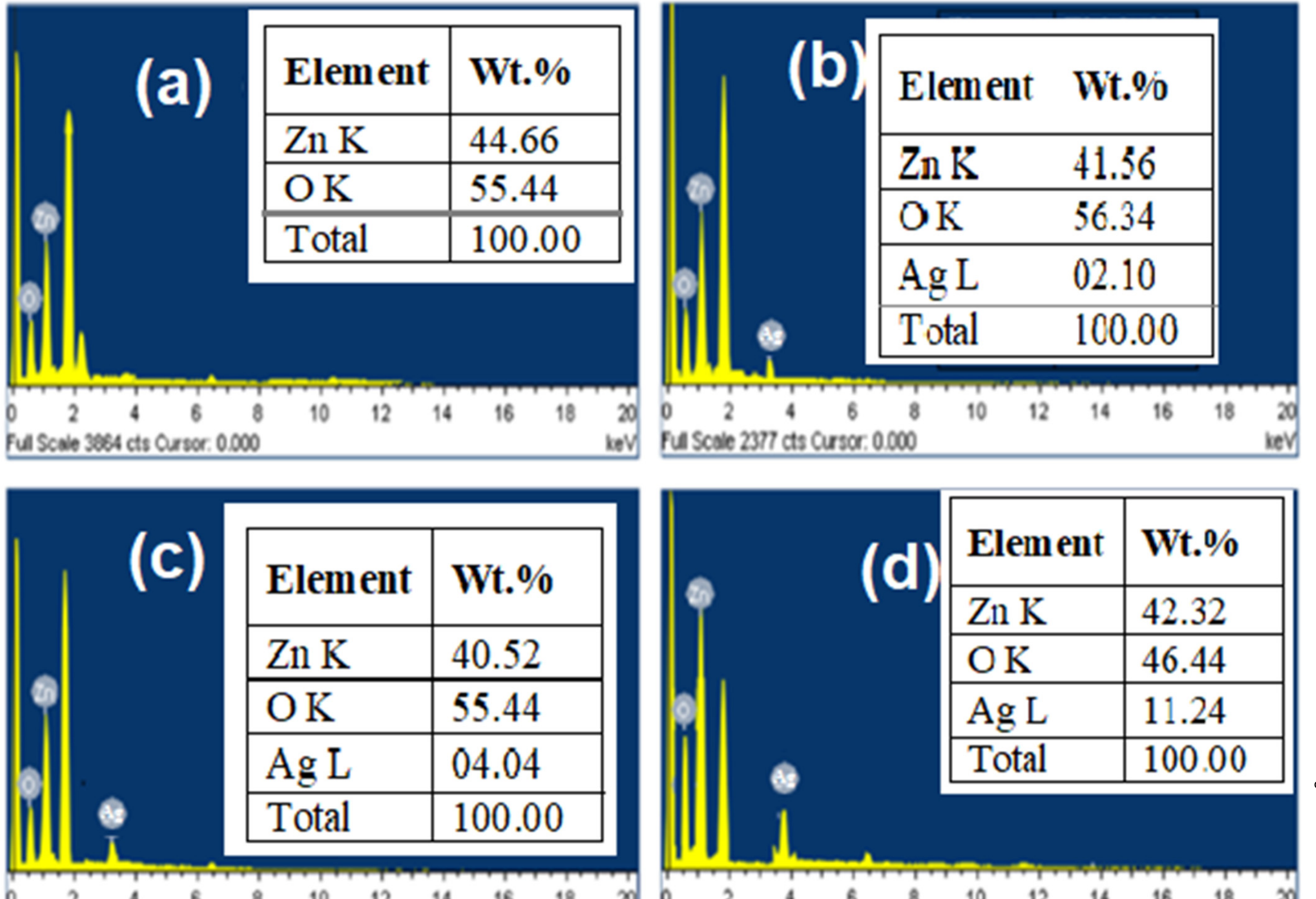

FIG. 4. EDX patterns of Ag/ZnO thin films at different Ag-sputter powers: (a) Ps(Ag) = 0 W, (b) Ps(Ag) = 90 W, (c) Ps(Ag) = 95 W, and (d) Ps(Ag) = 100 W. The patterns show the elemental composition of the films as influenced by varying sputter powers.

26 August 2024 13:47:53

in Ag-sputter power led to an increased transmittance of Ag/ZnO thin films up to 95 W. Each of the films had an easily identifiable and well-defined UV absorption edge, and all showed transmittance levels of about 75% in the visible range. Moreover, it was shown that a significant red shift in Ag/ZnO thin films occurs as the Ag-sputter increases.

To quantify the shift of the absorption edge, the thin films' bandgap energies were computed. Doped ZnO is known to be a

TABLE III. Comparison of various parameters of Ag/ZnO thin films at different Ag-sputter powers [Ps(Ag)]. This table provides a comprehensive overview of how parameters, such as optical, structural, and electrical properties, vary with changes in sputter power.

Sample	Method	Sputter power (W)	Transmittance (%)	Bandgap (eV)	Resistivity (Ω cm)	Reference
Ag-doped ZnO thin films	rf-magnetron sputtering	175	∼50	3.20	59.7×10^{-3} Ω cm	26
Ag-doped ZnO thin films	dc-magnetron sputtering	120	∼75	—	6 × 10−3 Ω cm	5
Ag/ZnS thin films	rf-magnetron sputtering	150	∼70	3.53	—	27
ZnO:Ag thin films	dc-magnetron cosputtering	100	—	—	60×10^{-3} Ω cm	11
Ag/ZnO thin films	dc-magnetron sputtering	95	82	3.24	0.8 Ω cm	Present work

Published under an exclusive license by the AVS

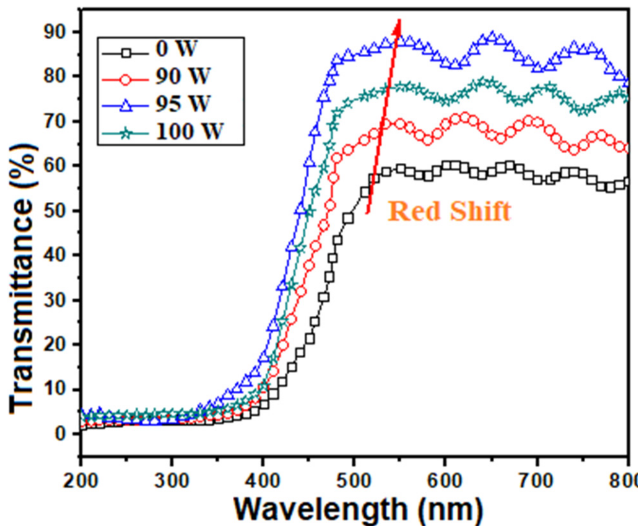

FIG. 5. Transmittance spectra of Ag/ZnO thin films at various Ag-sputter powers [Ps(Ag)]. The spectra illustrate the optical transparency of the films as a function of the sputter power.

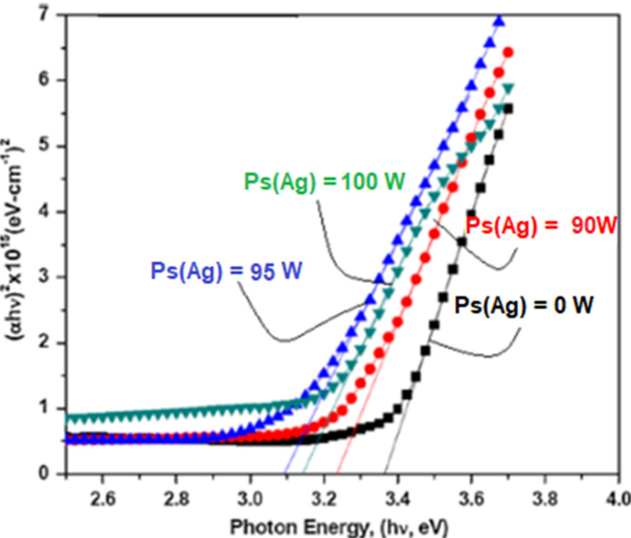

FIG. 6. $(\alpha h\nu)^2$ vs the hν plot of Ag/ZnO thin films at various Ag-sputter powers [Ps(Ag)]. The plot demonstrates the relationship between the photon energy and the absorption coefficient squared, indicating the optical bandgap of the films under different sputtering conditions.

wurtzite structure semiconductor with a direct band gap.[28] Therefore, the correlation between the absorption coefficient (α) and the photon energy (hν) for a direct transition could be expressed as[29]

$$(\alpha h\nu)^2 = (h\nu - E_g). \tag{2}$$

Both ZnO and Ag/ZnO are recognized as direct bandgap energy materials,[30] suggesting that Ag/ZnO can undergo direct allowed transitions. To determine the optical bandgap energy (E_g) of Ag/ZnO thin films at various Ag-sputter powers, extrapolate the linear section of the $(\alpha h\nu)^2$ versus (hν) plot to $\alpha = 0$ on the x axis, as illustrated in Fig. 6. This graphic provides the bandgap energies for all samples. When the 0 W Ag-sputter power yields an optical bandgap of about 3.3 eV, it means that the thin film contains only pristine ZnO and no Ag content. For Ag-sputter powers of 90, 95, and 100 W, the corresponding optical bandgap energy values are 3.24, 3.06, and 3.12 eV, respectively.

Figure 7 shows how the optical bandgap varies with Ag-sputter power. It is recognized that the noble metals, such as Ag, act as donors. Multiple research[31–33] on Ag/ZnO has consistently indicated that the insertion of Ag as a donor produces a red shift rather than a blue shift, indicating a decrease in the optical bandgap. It is noteworthy that isovalent doping of Ag in ZnO does not result in a new donor level. This implies that Ag/ZnO alloy's native flaws and complexes are the sole source of n-type carriers. The optical bandgap of Ag/ZnO thin films is minimal at 90 W. This is due to the substitution of zinc atoms by more silver atoms. Silver atoms integrate into crystal lattice sites and consequently decrease the bandgap as Ag-sputter power increases.[34] At higher Ag-sputter power (100 W), some Zn^{2+} and Ag^{2+} ions do not react with oxygen (O^{2-}) ions enough and do not penetrate into crystal lattice sites. Therefore, the optical bandgap decreases.

The variation of the refractive index (n) and the extinction coefficient (k) for the Ag/ZnO thin films as a function of wavelength in relation to Ag-sputter power is shown in Fig. 8. The

26 August 2024 13:47:53

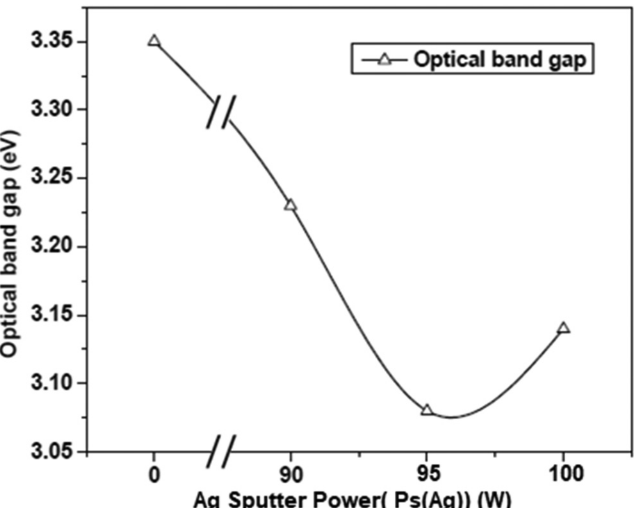

FIG. 7. Variation of optical band gap energy as a function of Ag-sputter power [Ps(Ag)]. This figure shows how the bandgap energy of Ag/ZnO thin films changes with different sputtering powers.

Published under an exclusive license by the AVS

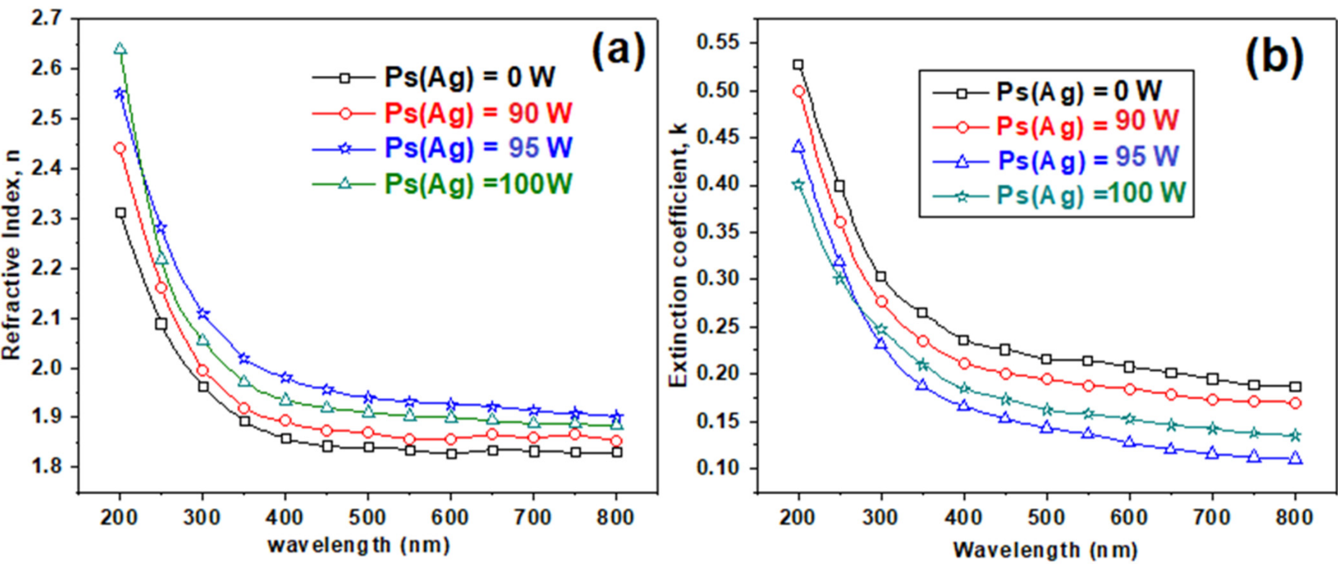

FIG. 8. Variation of the refractive index (n) (a) and the extinction coefficient (k) (b) of Ag/ZnO thin films as a function of Ag-sputter power [Ps(Ag)]. The figures illustrate how the optical constants of the films change with varying sputtering conditions.

above n and k of the films were calculated by using the following relations (3) and (4):[35]

$$n = \sqrt{N + \sqrt{(N^2 + n_0^2 n_1^2)}}, \quad (3)$$

where $N = (n_0^2 + n_1^2)/2 + 2n_0 n_1 (T_{\max} - T_{\min})/T_{\max} T_{\min}$,

$$k = \frac{\alpha\lambda}{4\pi}. \quad (4)$$

Relative flatness in the long wavelength region and a sharp increase in the shorter wavelength region are seen in the RI dispersion curves, which are indicative of normal dispersion in the films. When Ag-sputter power is increased to 95 W, the n shows an increase. This is followed by a minor fall that can be attributed to the reduction in the grain size. The n in the visible region varies from 2.0 to 1.82, which is in line with values published in the literature.[35] The reason for this uniformity could be the single-phase wurtzite structure found in thin films made of ZnO and Ag/ZnO. The optical losses due to absorption and scattering are included in the k, which progressively drops with decreasing wavelength. Ag/ZnO thin films have excellent surface smoothness, as indicated by the average k value in the visible range of 2×10^{-1}.[36] An indicative of the films' outstanding surface qualities is their low k, which is on the order of 10^{-1} in the visible region. Up to 95 W, the k falls as Ag-sputter power increases; after that, a loss in transmittance causes a little increase in k.

The electrical properties of the doped ZnO thin films are mainly dominated by the electrons generated by Zn interstitial

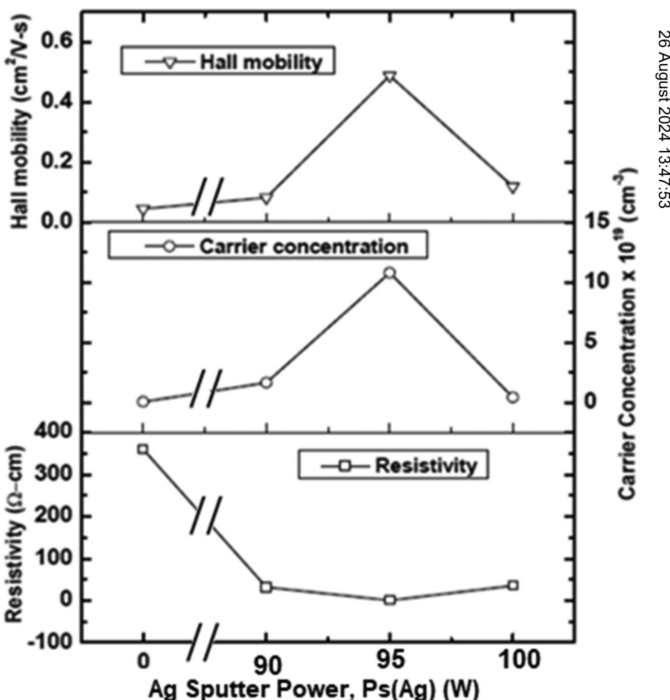

FIG. 9. Variation of electrical parameters: resistivity (ρ), carrier concentration (n), and Hall mobility (μ) in response to Ag-sputter power [Ps(Ag)]. This figure illustrates the impact of sputter power on the electrical properties of Ag/ZnO thin films.

26 August 2024 13:47:53

Published under an exclusive license by the AVS

atoms and oxygen vacancies.[37] Hall effect measurements were conducted using the van der Pauw method with the magnetic field of 0.5 T. The Hall measurements (ρ, n, and μ) of Ag/ZnO thin films at various Ag-sputter powers are depicted in Fig. 9. The resistivity (ρ) of the Ag/ZnO thin films is $3.45 \times 10^2\,\Omega\,\mathrm{cm}$ at an Ag-sputter power of 0 W. However, it dramatically decreases to a minimum of $0.8\,\Omega\,\mathrm{cm}$ at 95 W and then slightly increases to $10\,\Omega\,\mathrm{cm}$ at 100 W with the increasing Ag-sputter power. Hall electrical measurements indicate that all films exhibit n-type conductivity. Additionally, as the Ag-sputter power increased, the mobility (μ) roses from 0.05 to $0.48\,\mathrm{cm^2/V\,s}$. This corresponded to an increase in n from 9×10^{18} to $9.6 \times 10^{19}\,\mathrm{cm^{-3}}$, followed by a drop in both n and μ. As in many other MOSs, the mobility and carrier concentration of doped ZnO increases with increasing sputter power/pressure.[38] At lower Ag-sputter powers, the ρ of Ag/ZnO thin films exhibits quasi-intrinsic characteristics. The ρ is the lowest at 95 W Ag-sputter power, which is due to the bigger grain size. The rise in n and μ with sputter power, which is mostly due to an increase in the crystallite size, is demonstrated by GAXRD.

IV. CONCLUSIONS

In conclusion, this study demonstrates the successful fabrication of Ag/ZnO thin films through reactive dc/rf magnetron sputtering, with the sputter power being a key variable. A thorough exploration of the structural, surface, compositional, optical, and electrical properties of these films was conducted, revealing insights into the impact of Ag sputter power. The structural analysis, particularly via GAXRD studies, confirmed the presence of a single-phase hexagonal wurtzite ZnO structure in all films, predominantly oriented along the (002) direction. Notably, films deposited at 95 W Ag sputter power exhibited superior structural and morphological characteristics, featuring larger crystallites, minimal stress, and reduced roughness. The electrical properties revealed the n-type semiconducting nature of Ag/ZnO thin films, with a significant decrease in electrical resistivity, reaching a minimum of $0.8\,\Omega\,\mathrm{cm}$ at 95 W Ag sputter power. At this optimal power level, films displayed exceptional attributes, including low electrical resistivity, high mobility ($0.49\,\mathrm{cm^2/V\,s}$), a carrier concentration of $9.6 \times 10^{19}\,\mathrm{cm^{-3}}$, and high optical transmittance of 79%, accompanied by an optical bandgap energy of 3.06 eV. These findings underscore the crucial role of Ag sputter power in tailoring the properties of Ag/ZnO thin films for potential optoelectronic applications, offering insights for optimizing their performance in various device applications.

ACKNOWLEDGMENTS

The author A. GuruSampath Kumar would like to acknowledge the Inter-University Accelerator Centre, New Delhi for providing all the material characterization facilities (XRD, FE-SEM, AFM, UV-vis-N-IR Spectrophotometer, Hall Measurements, etc.) at IUAC Materials Science labs. We are also grateful to the Department of H&S (Physics), GRIET, Bachupally, Hyderabad 500090, Telangana, India for their necessary financial support.

AUTHOR DECLARATIONS

Conflict of Interest

The authors have no conflicts to disclose.

Author Contributions

GuruSampath Kumar A.: Conceptualization (equal); Data curation (equal); Formal analysis (equal); Investigation (equal); Methodology (equal); Software (equal); Supervision (equal); Writing – original draft (equal); Writing – review & editing (equal). **Mahender C.:** Data curation (equal); Formal analysis (equal); Investigation (equal); Methodology (equal); Writing – original draft (equal). **Mahesh Kumar U.:** Data curation (equal); Investigation (equal); Methodology (equal); Software (equal). **Obulapathi L.:** Data curation (equal); Investigation (equal); Methodology (equal); Writing – original draft (equal). **HemaChandra Rao B.:** Formal analysis (equal); Investigation (equal); Methodology (equal). **Yamuna P.:** Data curation (equal); Formal analysis (equal). **Thirupathi A.:** Data curation (equal); Formal analysis (equal). **SomaSundar L. N. V. H.:** Formal analysis (equal); Investigation (equal); Writing – original draft (equal). **Venkata Ramana G.:** Formal analysis (equal).

DATA AVAILABILITY

The data that support the findings of this study are available from the corresponding author upon reasonable request.

REFERENCES

[1]S. Usha and S. Suraj, J. Pure Appl. Phys. **10**, 10 (2022).
[2]M. Salem, H. Ghannam, A. Almohammedi, J. Salem, Y. Litaiem, I. Massoudi, M. Gassoumi, and M. Gaidi, Silicon **15**, 7321 (2023).
[3]I. López, L. Garza-Tovar, E. T. Adesuji, and M. Sanchez-Dominguez, "Colloidal core-shell metal, metal oxide nanocrystals, and their applications," in *Colloidal Metal Oxide Nanoparticles* (Elsevier, Netherlands, 2020), pp. 125–181.
[4]H. Krysova, V. Mansfeldova, H. Tarabkova, A. Pisarikova, Z. Hubicka, and L. Kavan, J. Solid State Electrochem. **28**, 2531 (2024).
[5]D. R. Sahu, Microelectron. J. **38**, 1252 (2007).
[6]D. J. Rani, A. GuruSampath Kumar, and T. S. Rao, J. Alloys Compd. **694**, 694 (2017).
[7]A. GuruSampath Kumar, T. Sofi Sarmash, L. Obulapathi, D. Jhansi Rani, T. Subba Rao, and K. Asokan, Thin Solid Films **605**, 102 (2016).
[8]S. H. Choe, Y. S. Kim, J. Y. Choi, Y. J. Park, B. C. Cha, Y. M. Kong, and D. Kim, Korean J. Met. Mater. **57**, 506 (2019).
[9]F. Lekoui, M. Ouchabane, H. Akkari, S. Hassani, and D. Dergham, Mater. Res. Express **5**, 106406 (2018).
[10]F. Lekoui, R. Amrani, S. Hassani, E. Garoudja, W. Filali, M. Ouchabane, N. Hendaoui, and S. Oussalah, Opt. Mater. **150**, 115151 (2024).
[11]R. Ramadan, S. Dadgostar, M. Manso –Silván, R. Pérez-Casero, M. Hernandez-Velez, J. Jimenez, and O. Sanchez, Mater. Sci. Eng. B **276**, 115558 (2022).
[12]G. O. Rabell, M. R. A. Cruz, and I. Juárez-Ramírez, Mater. Sci. Semicond. Process. **134**, 105985 (2021).
[13]A. Gurusampath Kumar, T. S. Sarmash, D. J. Rani, L. Obulapathi, G. V. V. B. Rao, T. S. Rao, and K. Asokan, J. Alloys Compd. **665**, 86 (2016).
[14]R. Swanepoel, J. Phys. E: Sci. Instr. **16**, 1214 (1983).
[15]A. GuruSampath Kumar, X. Li, Y. Du, Y. Geng, and X. Hong, Appl. Surf. Sci. **509**, 144770 (2020).
[16]Z. Ning, Y. Wang, S. Li, K. Tang, and M. Wen, Vacuum **210**, 111888 (2023).

26 August 2024 13:47:53

Published under an exclusive license by the AVS

[17]G. S. Kumar, X. Li, Y. Du, Y. Geng, and X. Hong, J. Alloys Compd. **798**, 467 (2019).
[18]S. K. Pendyala, K. Thyagarajan, A. G. Kumar, and L. Obulapathi, J. Microw. Power Electromagn. Energy **53**, 3 (2019).
[19]A. Thote *et al.*, ACS Appl. Electron. Mater. **1**, 389 (2019).
[20]D. J. Rani, A. G. S. Kumar, and T. S. Rao, J. Coat. Technol. Res. **14**, 971 (2017).
[21]D. J. Rani, A. G. S. Kumar, T. S. Sarmash, K. Chandra Babu Naidu, M. Maddaiah, and T. S. Rao, JOM **68**, 1647 (2016).
[22]S. Benramache, O. Belahssen, A. Arif, and A. Guettaf, Optik **125**, 1303 (2014).
[23]S. K. Esthappan, A. B. Nair, and R. Joseph, Compos. B Eng. **69**, 145 (2015).
[24]G. V. Vijaya Bhaskara Rao, U. Mahesh Kumar, L. N. V. H. Soma Sundar, K. Lakshmi Sarada, J. Vijay Kumar, A. GuruSampath Kumar, G. Venkata Ramana, B. H. Rao, L. Obulapathi, and X. Li, Braz. J. Phys. **54**, 120 (2024).
[25]S. Roy, S. Das, and C. K. Sarkar, Int. Nano Lett. **6**, 199 (2016).
[26]T. T. Ngoc Anh, T. Thi Ha, N. Viet Tuyen, and P. Nguyen Hai, VNU J. Sci.: Math. Phys. **35**, 87 (2019).
[27]X. Qu, R. Zhang, P. Zhang, X. Cao, R. Yu, and B. Wang, Opt. Mater. **148**, 114879 (2024).
[28]M. Karyaoui, D. Ben Jemia, M. Gannouni, I. Ben Assaker, A. Bardaoui, M. Amlouk, and R. Chtourou, Inorg. Chem. Commun. **119**, 108114 (2020).
[29]D. J. Rani, A. G. S. Kumar, L. Obulapathi, and T. S. Rao, IEEE Trans. Dielectr. Electr. Insul. **26**, 1134 (2019).
[30]H. Chen, Y. Qu, L. Sun, J. Peng, and J. Ding, Phys. E **114**, 113602 (2019).
[31]F. K. Shan, G. X. Liu, W. J. Lee, and B. C. Shin, J. Cryst. Growth **291**, 328 (2006).
[32]B. H. Rao, A. V. Rao, A. G. S. Kumar, and G. N. Rao, Dig. J. Nanomater. Biostructures **16**, 1173 (2021).
[33]A. G. Kumar, L. Xuejin, X. Hong, Y. Geng, Y. Du, and T. S. Rao, Radiat. Phys. Chem. **162**, 107 (2019).
[34]N. M. Rohith, P. Kathirvel, S. Saravanakumar, and L. Mohan, Optik **172**, 940 (2018).
[35]D. J. Borah, A. T. T. Mostako, P. K. Saikia, and P. Dutta, Mater. Sci. Semicond. Process. **93**, 111 (2019).
[36]H.-B. Kim and J.-J. Kim, Opt. Express **28**, 11892 (2020).
[37]N. Najafi and S. M. Rozati, Mater. Res. **21**, e20170933 (2018).
[38]C. H. Tseng, W. H. Wang, H. C. Chang, C. P. Chou, and C. Y. Hsu, Vacuum **85**, 263 (2010).

26 August 2024 13:47:53

Published under an exclusive license by the AVS